doi:10.1111/evo.12207

# SHIFTING FITNESS LANDSCAPES IN RESPONSE TO ALTERED ENVIRONMENTS

**Ryan T. Hietpas,[1,*] Claudia Bank,[2,3,*] Jeffrey D. Jensen,[2,3,4,†] and Daniel N. A. Bolon[1,5,†]**

[1]*Department of Biochemistry and Molecular Pharmacology, University of Massachusetts Medical School, Worcester, Massachusetts, 01605*

[2]*School of Life Sciences, École Polytechnique Fédérale de Lausanne, 1015 Lausanne, Switzerland*

[3]*Swiss Institute of Bioinformatics (SIB), 1015 Lausanne, Switzerland*

[4]*E-mail: Jeffrey.Jensen@epfl.ch*

[5]*E-mail: Dan.Bolon@umassmed.edu*

Received March 28, 2013
Accepted June 25, 2013
*Data Archived: Dryad doi: 10.5061/dryad.nb259*

**The role of adaptation in molecular evolution has been contentious for decades. Here, we shed light on the adaptive potential in Saccharomyces cerevisiae by presenting systematic fitness measurements for all possible point mutations in a region of Hsp90 under four environmental conditions. Under elevated salinity, we observe numerous beneficial mutations with growth advantages up to 7% relative to the wild type. All of these beneficial mutations were observed to be associated with high costs of adaptation. We thus demonstrate that an essential protein can harbor adaptive potential upon an environmental challenge, and report a remarkable fit of the data to a version of Fisher's geometric model that focuses on the fitness trade-offs between mutations in different environments.**

**KEY WORDS:** **Adaptation, adaptive walk, distribution of fitness effects, experimental evolution, Fisher's geometric model.**

As multiple whole genome projects come to fruition, the presence of whole genome data within and between populations and species has spurred the development of a large class of test statistics aimed at describing the distribution of fitness effects (DFE), or some aspect of the distribution, using polymorphism and divergence data (Eyre-Walker et al. 2006; Li and Stephan 2006; Andolfatto 2007; Keightley and Eyre-Walker 2007; Macpherson et al. 2007; Boyko et al. 2008; Jensen et al. 2008). Yet, the abundance of empirical, theoretical, and computational study has led to contentious findings. Turning to perhaps the best-studied organism in population genetics, Drosophila melanogaster—estimates are far from consistent, and reconciling results with one another is often challenging. For example, considering polymorphism data, Li and Stephan (2006) and Jensen et al. (2008) estimate the mean beneficial selection coefficient (s) at 0.002, whereas Macpherson et al. (2008) estimate at 0.01, and Andolfatto (2007) at 0.00001.

Considering other avenues for illuminating the DFE apart from statistical inference, we come to the rich field of experimental evolution. These studies have often come in the form of mutation accumulation experiments—with most results recapitulating the basic expectations of Timofeeff-Ressovsky (1940) and Muller (1950), that most mutations which affect phenotype must be strongly deleterious owing to billions of years of gradual improvements. However, one of the main limitations of such experiments derives from the structure itself. Observations are limited to considering only mutations that happen to spontaneously occur, and are generally focused upon characterizing the rate of accumulation of deleterious variants. In recent years, panels of tens to hundreds of spontaneous or engineered (Eyre-Walker and Keightley 2007) mutants have been investigated for their impacts on fitness under variable conditions in both bacteria (Kassen

*These authors contributed equally to this work.
†Co-corresponding authors.




EVOLUTION
INTERNATIONAL JOURNAL OF ORGANIC EVOLUTION

and Bataillon 2006; MacLean and Buckling 2009; Schenk et al. 2012; Trindade et al. 2012) and viruses (Lalic et al. 2011; Vale et al. 2012). These studies have provided important insights into the environmental dependence of mutant fitness effects. However, precise measurement of fitness effects for large panels of mutants in an otherwise identical genetic background and under distinct environmental conditions remains an arduous challenge.

To overcome many of these limitations, Hietpas et al. (2011) recently proposed a methodology coined "extremely methodical and parallel investigation of randomized individual codons" (EMPIRIC)—which generates high-quality systematic mutant libraries and measures fitness with a large dynamic range. The EMPIRIC approach enables the investigation of all possible point mutations (and their effect relative to wild type) for a given region. This has the advantage of mutation accumulation experiments inasmuch as the DFE of new mutations may be directly observed, rather than inferred from the distribution of segregating and fixed mutations, but has the additional benefit of allowing for a systematic exploration of the full mutational landscape for regions of genes. We developed EMPIRIC to provide precise and reproducible measurements of individual mutations including performing experiments with yeast rapidly expanded from a single colony to provide a homogeneous genetic background, maintaining large populations throughout to minimize stochastic fluctuations in mutant frequencies, and including the wild-type sequence in our competitions to provide a direct reference. Thus our approach avoids pitfalls common to previous bulk competitions (Manna et al. 2012). Given the experimental procedure, a given identical mutation (on an identical genetic background) may be readily compared across multiple environments. This benefit however comes at the cost of two distinct trade-offs: (1) we here focus on a specific genomic region, rather than the whole-genome search associated with mutation accumulation experiments, and (2) the experimentally controlled environment is not necessarily related to the complex and variable environmental pressures experienced by natural populations.

We focused our analyses of environmental conditions on two parameters (temperature and salinity) expected to affect the biophysical and biochemical properties of multiple proteins and hence to place distinct pressures on the Hsp90 chaperone system. As its name indicates, heat shock protein 90 is a chaperone that is upregulated in response to elevated temperature (McKenzie et al. 1975). Heat-induced expression of Hsp90 in yeast is required for efficient growth at temperatures above 37°C (Borkovich et al. 1989). Genome-wide analyses of mRNA abundance indicate that Hsp90 is transiently upregulated upon heat shock at 37°C with a maximum eightfold response after 10 min, but in steady-state growth at this temperature it is not significantly upregulated (Gasch et al. 2000). In addition, Hsp90 regulates the global transcriptional response to elevated temperature by binding to heat shock factor 1 (HSF1). Under normal conditions, Hsp90 binds to HSF1 keeping it in an inactive state. Elevated temperature causes Hsp90 to release HSF1 that triggers the main transcriptional response to heat shock (Zou et al. 1998).

In contrast to Hsp90's central role in the response to heat stress, it plays a more modest role in the response to osmotic stress. For example, elevated salinity (0.7 or 1 M sodium chloride) does not cause a statistically significant change in Hsp90 mRNA levels in yeast over either short or long time periods (Gasch et al. 2000; Causton et al. 2001; Berry and Gasch 2008). Although Hsp90 is not upregulated in response to elevated salinity, its basal function is required for robust growth under hyperosmotic conditions (Yang et al. 2006). Indeed Hsp90 and its co-chaperone Cdc37 are both required for activation of the high osmolarity glycerol pathway (Hawle et al. 2007; Yang et al. 2007) that yeast require for growth under conditions of elevated salinity (Hohmann 2002). Although Hsp90 function is intimately linked to the yeast response to elevated temperature, it plays a more indirect role in the yeast response to elevated salinity.

In the initial study (Hietpas et al. 2011), considering a strongly conserved region of a strongly conserved gene (Hsp90, an essential chaperone in eukaryotes [Borkovich et al. 1989] required for the maturation of many kinases [Whitesell et al. 1994; Whitesell and Lindquist 2005]), results were quite clear—with a strong bimodal distribution containing mutations nearly equivalent to wild type, mutations that were strongly deleterious, and no observed beneficial mutations. We made the case that this observation was remarkably consistent with Ohta's (1971) expectation under the nearly neutral model. However, this first proof-of-principle study may in some ways be regarded as the most likely scenario for replicating the predictions of the nearly neutral model—in that, given the gentle growth conditions and the evolutionary importance of this region—it might be considered unlikely to identify mutations more fit than wild type for the reasons argued by Muller (1950).

One valuable approach for interpreting unique data of this type is within the context of Fisher's geometric model (FGM) (Fisher 1930)—a widely used framework for interpreting adaptation to novel environments—which yields expectations of the proportion of beneficial to deleterious mutations, as well as the mutational steps sizes and distances characterizing adaptive walks (Orr 1998, 2003). The comparison of evolutionary models with experimental measures has a rich tradition (e.g., examining the underlying causes of epistasis [Martin et al. 2007]). For interpreting our data, the FGM provides an intuitive framework for quantifying the cost of adaptation. The model itself is straightforward (see also Fig. 1 in Orr 1998). For a given environment, the fitness of an individual is characterized by its position in an $n$-dimensional phenotype space. Fitness is assumed to decrease radially from a single phenotypic optimum. Hence, the Euclidean

distance to the optimum determines the fitness of an individual. Random vectors originating from the current phenotype represent new mutations. Those mutations that decrease the distance to the optimum are considered beneficial and can hence contribute to adaptation, whereas those that increase the distance to the optimum are considered deleterious. The better the current phenotype is adapted to the environment, the closer it is to the phenotypic optimum. Thus, for a population near optimum, fewer mutations are expected to be beneficial, because, by solely geometrical arguments, the probability that a randomly occurring mutation will decrease the distance to the optimum becomes lower as the optimum nears. Different environments correspond to differently located optima in phenotype space. The position of each of these optima (relative to one another, and the current phenotype) determines the number and magnitude of beneficial mutations and the expected cost of adaptation between different environments. Of note, the FGM inherently proposes (potentially high) costs of adaptation: as soon as the phenotypic optimum is relocated upon a change in environment, subsets of the phenotype space arise in which mutations are beneficial in one environment while deleterious in the other.

Continuing to exploit the EMPIRIC high-throughput approach, we examine changes in the DFE for a region of the Hsp90 gene in associated with novel selective pressures—here in the form of variations in temperature and salinity. We uniquely address two general and long-standing points of both theoretical and empirical interest: (1) the applicability of FGM (Fisher 1930) for populations facing adaptive challenges, and (2) a characterization of the relative cost of adaptation.

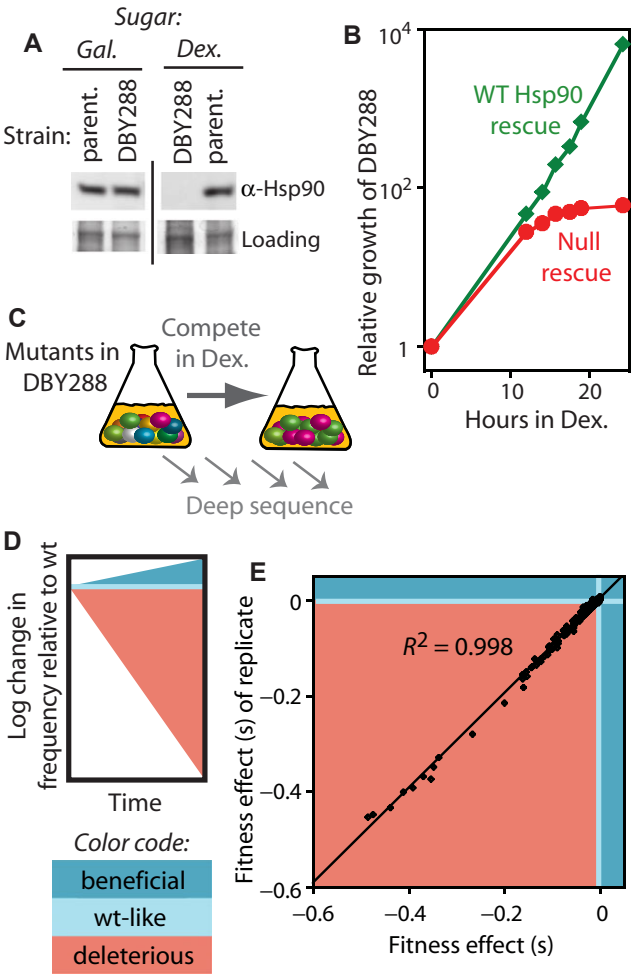


**Figure 1.** EMPIRIC fitness analyses in a shutoff strain. The yeast strain DBY288 was engineered to express Hsp90 at endogenous levels when grown in galactose medium, and shutoff in dextrose medium, confirmed by Western analysis in (A). Growth of DBY288 yeast in dextrose was rescued with a plasmid that constitutively expresses Hsp90 (B). To measure fitness effects of mutants, systematic point mutant libraries were competed in bulk with deep sequencing used to readout the abundance of each mutant (C). The time-dependent change in mutant frequency provided a direct examination of relative growth (D). This approach provided precise and reproducible measurements of fitness effects (E).

## Materials and Methods

### PLASMID LIBRARY CONSTRUCTION

Saturative single codon substitution libraries of amino acids 582–590 were generated in plasmid p417GPD that constitutively expresses Hsp90 as previously described (Hietpas et al. 2011).

### YEAST TRANSFORMATION AND SELECTION

Constitutively expressed libraries of Hsp90 mutants were introduced into a shutoff strain, amplified in galactose media, and then competed in dextrose media. These studies used the DBY288 yeast strain (can1–100 ade2–1 his3–11,15 leu2–3,12 trp1–1 ura3–1 hsp82::leu2 hsc82::leu2 ho::pgals-hsp82-his3) where expression of the only Hsp90 gene in these cells strictly depends on galactose. A single colony of DBY288 was picked from a synthetic raffinose/galactose (Gal) plate and inoculated into 25 mL 2× YPA Gal medium (20 g yeast extract, 40 g peptone, and 0.2 g adenine hemisulphate per liter with 1% (w/v) raffinose and 1% galactose) and grown at 30°C on an orbital shaker to late log phase. The culture density was calculated by hemocytometry and $10^8$ cells were inoculated into 50 mL of fresh 2× YPA Gal medium. The culture was grown for 5 h at 30°C with agitation, harvested by centrifugation at 3000 × g for 5 min and transformed by the standard lithium acetate protocol (Gietz et al. 1995; Gietz and Schiestl 2007) with plasmid (either mutant libraries, a positive control with wild-type Hsp90, or negative control lacking Hsp90). The generation time of cells harboring wild-type Hsp90 was determined by following the change in optical density over time (Fig. S1). To examine measurement precision, replicate competition experiments were performed under the 30°C condition with cultures split after transformation (Fig. 1E).

After heat shock at 42°C for 30 min, the cells were pelleted at 3000 × g for 5 min and washed twice with 500 μL Gal medium (1.7 g yeast nitrogen base without amino acids, 5 g ammonium sulfate, 0.1 g aspartic acid, 0.02 g arginine, 0.03 g valine, 0.1 g glutamic acid, 0.4 g serine, 0.2 g threonine, 0.03 g isoleucine, 0.05 g phenylalanine, 0.03 g tyrosine, 0.04 g adenine hemisulfate, 0.02 g methionine, 0.1 g leucine, 0.03 g lysine, 0.01 g uracil per liter with 1% raffinose and 1% galactose) and recovered in 5 mL Gal medium for 16 h. The cells were pelleted by centrifugation at 3000 × g for 5 min and inoculated into 50 mL Gal medium with 200 μg/mL G418. The culture was then allowed to grow at 30°C on an orbital shaker to near saturation (about 48 h). Twenty milliliters of this culture was washed with fresh Gal medium and the pellet was inoculated into 100 mL synthetic Gal medium containing 100 μg/mL ampicillin. This culture was grown for 12 h in log phase, diluting when necessary. The log phase cells were then inoculated to an $OD_{600}$ of ∼0.1 in 150 mL of synthetic dextrose (Dex) medium (identical composition to Gal media except with 2% dextrose as the sugar source) with 100 μg/mL ampicillin that were grown at 30°C on an orbital shaker. After 8 h, the culture was split into four different environmental conditions (30°C, 36°C, 30°C + S, 36°C + S; where S represents the addition of 0.5 M sodium chloride). The culture was then grown for 12–20 generations in log phase (diluting when needed). Samples were reserved at different time points throughout the experiment by pelleting $10^9$ cells and storing the pellets at −80°C.

## DNA PREPARATION, SEQUENCING, AND ANALYSIS

Yeast lysis, DNA preparation, and sequencing was performed as described (Hietpas et al. 2012). Sequencing was performed by the UMass deep sequencing core facility, and generated ∼30 million reads of 99% confidence at each read position as judged by PHRED scoring (Ewing and Green 1998; Ewing et al. 1998). The relative abundance of each mutant relative to wild type was calculated at each sampled time point. The slope of the logarithm of relative mutant abundance versus time in generations was used as a direct measure of relative fitness. To account for sequencing noise, an outlier detection based on the box-plot rule was performed for each mutant's trajectory—hence, datapoints outside the range spanned by the 50% confidence interval extended by 1.5 times the interquartile range on each side were excluded from the linear regression. To obtain normalized selection coefficients for each dataset such that wild-type (wt) fitness represents $s = 0$, we selected all mutants that result in wild-type synonyms as a reference set and calculated its mean and standard deviation. To account for potential outliers of the distribution of synonyms, we neglected those mutations further than two standard deviations away from the mean, and defined the resulting new mean as the normalization constant representing $s = 0$. Hence, each selection

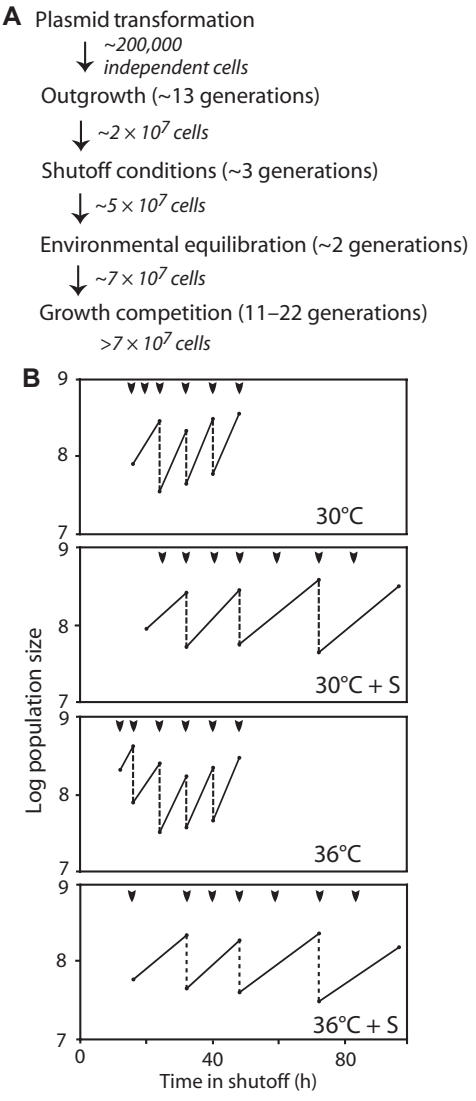


**Figure 2. Population management during bulk competition experiments. (A) Complete experimental outline from initial transformation. The number of independent transformants and minimum population sizes during all phases of growth were in gross excess to the diversity of our library containing 567 mutants. (B) Trajectories indicating population sizes during the selection phase in each environmental condition. Dashed lines indicate dilutions, arrowheads indicate time points harvested and used for calculation of fitness.**

coefficient on the nucleotide level is calculated as the slope of its absolute read numbers minus the normalization constant. The selection coefficient of each amino acid is thereupon obtained as a weighted average of the selection coefficients of all synonymous codons. Weights are assigned after outlier detection (according to the box-plot rule) on the time-point level to account for the effect of low read numbers in the initial library. For Figure 2, mutations were categorized as indistinguishable from wild type (wt-like) if $|s| < 0.01$, beneficial if $s > 0.01$, deleterious if $-0.01 > s > -0.5$, and strongly deleterious if $s < -0.5$. The threshold for the

wt-like category represents a strongly conservative choice to assure that beneficial mutations are truly advantageous—however, we observed no qualitative differences in the results when this threshold is set to $|s| < 0.005$.

### REPRODUCIBILITY OF FITNESS EFFECTS IN A BULK COMPETITION REPLICATE

To further investigate potential fitness contributions from background mutations in pools of transformed cells and to vet the reproducibility of bulk fitness measurements, we performed a subsequent full experimental replicate under 30°C + S conditions that included separate transformations. DBY288 cells were transformed and selected as in the original experiment at 30°C + S. Mutants with fitness effects $s > -0.2$ were compared between full experimental replicates (Fig. S3) and exhibited a high level of reproducibility ($R^2 = 0.97$).

### CONFIRMATION OF MUTANT FITNESS EFFECTS BY BINARY COMPETITION

To confirm the fitness measurement generated by the EMPIRIC approach, we developed an independent qPCR based assay to measure the fitness of a subset of mutants by binary competition (Figs. S4 and S5). The binary competition assays competed cells bearing a single point mutant against cells bearing wild-type plasmid. A 50 bp region was inserted into a noncoding region of the wild-type plasmid to distinguish mutant from wild type. This insertion did not alter the growth property of the host strain, but did enable quantification of the relative abundance of wild type and mutant cells in binary competitions. Wild type and point mutant plasmid were mixed at a 1:1 molar ratio and cotransformed into DBY288 cells. Growth, selection, and lysis procedures were identical to the EMPIRIC experiment. For qPCR analysis, a common reverse primer and a wild-type or mutant-specific forward primer was used produce a 300 bp amplicon. The qPCR reactions consisted of the following: 1× SYBR Green I gel stain, 500 nM each forward and reverse primer, 50 μM each dNTP, 1× Phusion HF buffer, 0.5 mM additional magnesium chloride, 0.5 μL Phusion DNA polymerase, in a final volume of 50 μL. PCR conditions were as follows: 94°C for 2 min; 40 cycles of 94°C for 30 s, 59.5°C for 30 s, 72°C for 30 s. Standard curves were generated by analyzing dilution series (1–$10^{-4}$ ng) of wild type and mutant plasmids with both primer sets in triplicate. Experimental samples contained 1–2 μL of lysate as template with equal volumes amplified with each primer set. Selection coefficient measurements were repeated in triplicate to assess measurement precision.

### CORRESPONDENCE WITH THE FITNESS TRADE-OFFS PREDICTED BY THE FGM

Given four environments and a straightforward distinction of two classes of mutations (beneficial if $s > 0$, deleterious if $s < 0$) in each environment, there are $2^4 = 16$ possible categories of mutations, ranging from "deleterious in all environments" to "beneficial in all environments." From Martin and Lenormand (2006a), equation (4a), one can determine the effective number of phenotypic dimensions in the FGM as $n_e = 2E(s)^2/V(s)$, where $E(s)$ and $V(s)$ are the mean and the variance of the distribution of deleterious (but not lethal) mutation effects in a population that is close to the optimum (in our experiment corresponding to all mutations with $-0.5 < s < 0$ from 30°C). We obtain $n_e \approx 1.08$, clearly supporting a one-dimensional phenotype space. Despite being restricted to a small region of a single protein, our data are in agreement with whole-genome estimates from mutation accumulation experiments (Martin and Lenormand 2006a). Even though the theory was developed for populations close to the optimum, we obtain similar numbers for the high-salinity environments (30°C + S: $n_e = 0.80$; 36°C + S: $n_e = 1.40$), whereas the result from the high-temperature environment would indicate a higher complexity of its phenotype space (36°C: $n_e = 2.79$).

We estimated the distance to the optimum in each environment by fitting a shifted gamma distribution following Martin and Lenormand (2006b) (see eq. 5), by neglecting the strongly deleterious mode of the distribution. Its location parameter $s_0$ determines the distance to the optimum. We obtain $s_0 = 0.007$ for 30°C, $s_0 = 0.002$ for 36°C, $s_0 = 0.087$ for 30°C + S, and $s_0 = 0.045$ for 36°C + S. Notably, the same ranking and similar proportions are obtained if the mean, median, or the maximum of all beneficial mutations are taken as reference for the distance to the optimum. For combinatorial reasons, there exist eight different geometric arrangements of the four optima in phenotype space that each contain five categories of mutations (cf. Fig. 5). We identify the best fit in accordance with the FGM (shown in Fig. 4) to harbor 181/189 (= 95.8%) of all mutations. The 189 amino acid substitutions represent all 20 amino acids plus stop codons at nine positions. Fitness measurements of amino acid substitutions were averaged over synonymous substitutions resulting in independent measures of the wild-type amino acid at each position. Classifications according to the best fit are shown in the last column of Data S1, labeled as indicated in Fig. 4 (additionally, the label "I" represents incongruous mutations). Note that all but one of the incongruous mutations can be classified if the sign of wt-like mutations is neglected (hence, incongruity is likely explained by the limits of accuracy of the experiment).

## *Results and Discussion*

To facilitate fitness analyses of Hsp90 mutants under varied temperature and salinity, we created the DBY288 shutoff strain. In this strain, the only chromosomal copy of Hsp90 is driven by a

strictly galactose-dependent promoter. In galactose (Gal) media this strain expresses Hsp90 to a level similar to the parental strain, but in dextrose (Dex) media Hsp90 expression is fully shut off (Fig. 1A). Transformation of this strain with a plasmid that constitutively expresses Hsp90 rescues growth in dextrose compared to a control plasmid lacking Hsp90 (Fig. 1B). This conditional strain allows libraries of Hsp90 mutants to be amplified in Gal media, and then competed in Dex media where growth depends on the function of the library Hsp90 variants. Importantly, these bulk competitions can be performed under conditions of varied temperature and salinity.

We analyzed mutants in a region encompassing amino acids 582–590 of Hsp90. This region forms a hydrophobic patch on the surface of the Hsp90 structure including F583 and W585 that forms a putative substrate binding site (Harris et al. 2004), and that we speculate has the potential to impact client maturation as a function of distinct environments. We transformed a systematic library of mutations including all possible point mutations in this region into the DBY288 strain, amplified the resulting yeast library in Gal media, and performed a bulk competition in Dex medium (Fig. 1C) under four different conditions (30°C, 36°C, 30°C + S, 36°C + S, where +S indicates elevated salinity). For cells harboring wild-type Hsp90, both elevated temperature and salinity reduced growth rate with the combined 36°C + S condition causing the greatest reduction (Fig. S1), indicating a greater joint stress.

The relative abundance of each mutant in bulk competition was determined by focused deep sequencing of samples extracted from the culture over time (Fig. 1C). The change over time in relative abundance of an amino acid substitution relative to the wt amino acid (Fig. 1D) yields a direct readout of the relative fitness effect of each point mutant in the library. Importantly, each point mutant is analyzed with precise control over genetic background and environmental sampling relative to all other mutants because the library is transformed into the same batch of yeast, and the bulk competitions are performed in the same flask where rapid mixing ensures that all mutants experience identical conditions. The ability to standardize genetic background and environmental conditions results in measurements of fitness effects that are highly reproducible (Fig. 1E). The precision of these measurements enables unique systematic exploration of the DFEs that we have analyzed with regard to expectations from FGM.

Experimental competitions under each environmental condition were managed to provide robust fitness measurements (Fig. 2). To limit stochastic fluctuations, population sizes were maintained in gross excess to the diversity of our libraries at all steps. In addition, cells were analyzed rapidly once subject to selective conditions to limit the influence of potential secondary mutations. With these safeguards in place we analyzed the fitness effects of mutations under conditions of elevated temperature and/or elevated salinity (Fig. 3, Supporting Data S1). Compared to the standard condition (0 mutations with $s > 0.01$; $s_{max} = 0.007$), we observe a dramatic increase in the number and magnitude of beneficial mutations in Hsp90 under conditions of elevated salinity (in 30°C + S: 38 mutations with $s > 0.01$, $s_{max} = 0.083$; in 36°C + S: 24 mutations with $s > 0.01$; $s_{max} = 0.044$).

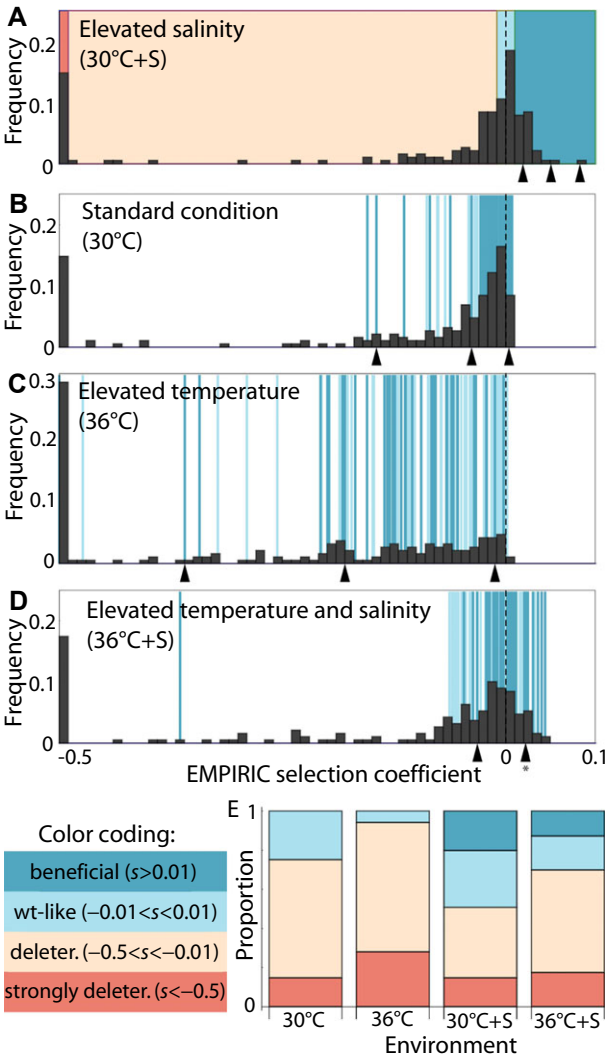


**Figure 3.** **Fitness of mutants in different environments. (A) Histogram of mutant fitness in 30°C + S. To exemplify the costs of adaptation to elevated salinity, the fitness effects of the beneficial (dark blue area) and wild-type-like (light blue area) mutations identified in 30°C + S are indicated as dark and light blue bars in the corresponding histograms in 30°C (B), 36°C (C), and 36°C + S (D). The selection coefficients of three independently validated beneficial mutations in 30°C + S and their corresponding selection coefficients in the other environments are indicated by black triangles (Two overlapping triangles in (D) are marked with a star). (E) Proportions of beneficial, wild-type-like, deleterious, and strongly deleterious mutations in the different environments.**

As recent studies have observed that the adaptation of yeast to new conditions can be dramatically influenced by standing mutations (Gresham et al. 2008), and mutations to multiple adaptive mutational pathways have been reported for yeast in elevated salinity (Dhar et al. 2011), we took additional steps to ensure that the observed beneficial fitness effects (Fig. 3) were caused by the specifically induced amino acid changes in Hsp90. First, we analyzed synonymous substitutions underlying the identified beneficial amino acid, as most were encoded by multiple codons (e.g., N588P is encoded by four separate nucleotide variants). During transformation, each codon variant should enter a distinct pool of cells. If adaptation were primarily driven by secondary mutations within the genomes of these pools of cells, we would expect to observe highly variable fitness measurements among codons of the same amino acid. In contrast, if adaptation is primarily due to the Hsp90 amino acid substitution, then synonymous substitutions should have a narrow distribution. Among the beneficial amino acids that we observe, the DFEs for synonymous codons are indeed narrow (Fig. S2), indicating that the induced mutations in Hsp90 are the primary determinant underlying the experimental observation. Second, we performed a follow-up 30°C + S study with two experimental replicates using independent transformations. In these experiments, we observe a similar number of beneficial mutations and a strong correlation between each independent replicate (Fig. S3). Third, we developed a qPCR based binary competition (Fig. S4) that we used as an alternative strategy to measure fitness effects of six individual mutations (Fig. S5). The fitness effects observed by binary competition correlate well with those measured by EMPIRIC bulk competitions. From this collection of experiments, we conclude that our fitness measures are primarily owing to the induced amino acid changes.

We studied the DFEs along two environmental axes comprising elevated temperature and elevated salinity. These are associated with different expectations concerning the potential for adaptation and the distance to the optimum in the FGM. As a heat shock protein, Hsp90 is per definition suited to cope with elevated temperature, and its function becomes even more essential upon heat stress as discussed above. Hence, we hypothesize that the endogenous sequence is close to the phenotypic optimum under high temperature and beneficial mutations rare. In contrast, we hypothesize that elevated salinity may pose a novel environmental challenge that is not directly associated with the function of Hsp90. Therefore, we expect a relocation of the phenotypic optimum that yields increased potential for adaptation.

The above expectations are clearly supported by our results: both under standard conditions (30°C) and under elevated temperature (36°C) we find no beneficial mutations, indicating that the current phenotype is close to the phenotypic optimum (cf. Fig. 3B,C). In contrast, we find numerous beneficial mutations

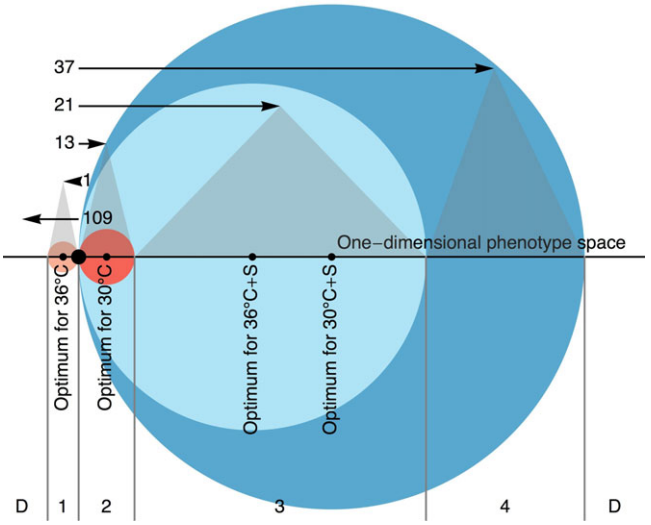


**Figure 4.** Graphical representation of the fit of the FGM. The horizontal black solid line represents the one-dimensional phenotype space, on which the big black dot indicates the position of the current phenotype. For each environment, a colored circle (evocative of the original two-dimensional picture of the FGM [cf. Fig. 1, Orr 1998]) is drawn tangential to the current phenotype with its radius corresponding to the distance to the phenotypic optimum (indicated as indexed small black dot) of the respective environment. The interval corresponding to the projection of each circle onto the one-dimensional phenotype space represents the area into which mutations have to fall according to the FGM to decrease the distance to the optimum and hence to be beneficial in a particular environment. A total of 181 of 189 analyzed mutations are in agreement with a one-dimensional FGM, in which the distance of the current phenotype to the optimum for each environment in phenotype space is assumed to rank according to the selection coefficient of the most beneficial mutation (here, the radius of the circles is drawn proportional to the selection coefficient of the best mutant). This yields five categories of mutations that are characterized by the overlap of the projected circles (cf. also Fig. 5): (D) Deleterious in all environments, (1) $s > 0$ in 36°C only, (2) $s < 0$ in 36°C only, (3) $s < 0$ in 30°C and 36°C; $s > 0$ in 30°C + S and 36°C + S, (4) $s > 0$ in 36°C + S only. Arrows represent exemplary mutations for each of these categories, indexed with the respective observed number of such mutations per category. Gray triangles indicate the projection of these categories onto the respective interval in phenotype space (see also Fig. 5).

under elevated salinity (30°C + S) and under combined elevated temperature and salinity (36°C + S, cf. Fig. 3A,D). As hypothesized, the proportion of deleterious mutations grows with increased heat stress in the 36°C and 36°C + S environments as compared with 30°C (Fig. 3E). In addition, Fig. 3E shows that the proportion of beneficial mutations under high salinity is reduced upon increased heat stress, indicating that the current phenotype is closer to the phenotypic optimum in 36°C + S than in 30°C + S—which is supported by the estimated distances to the optimum

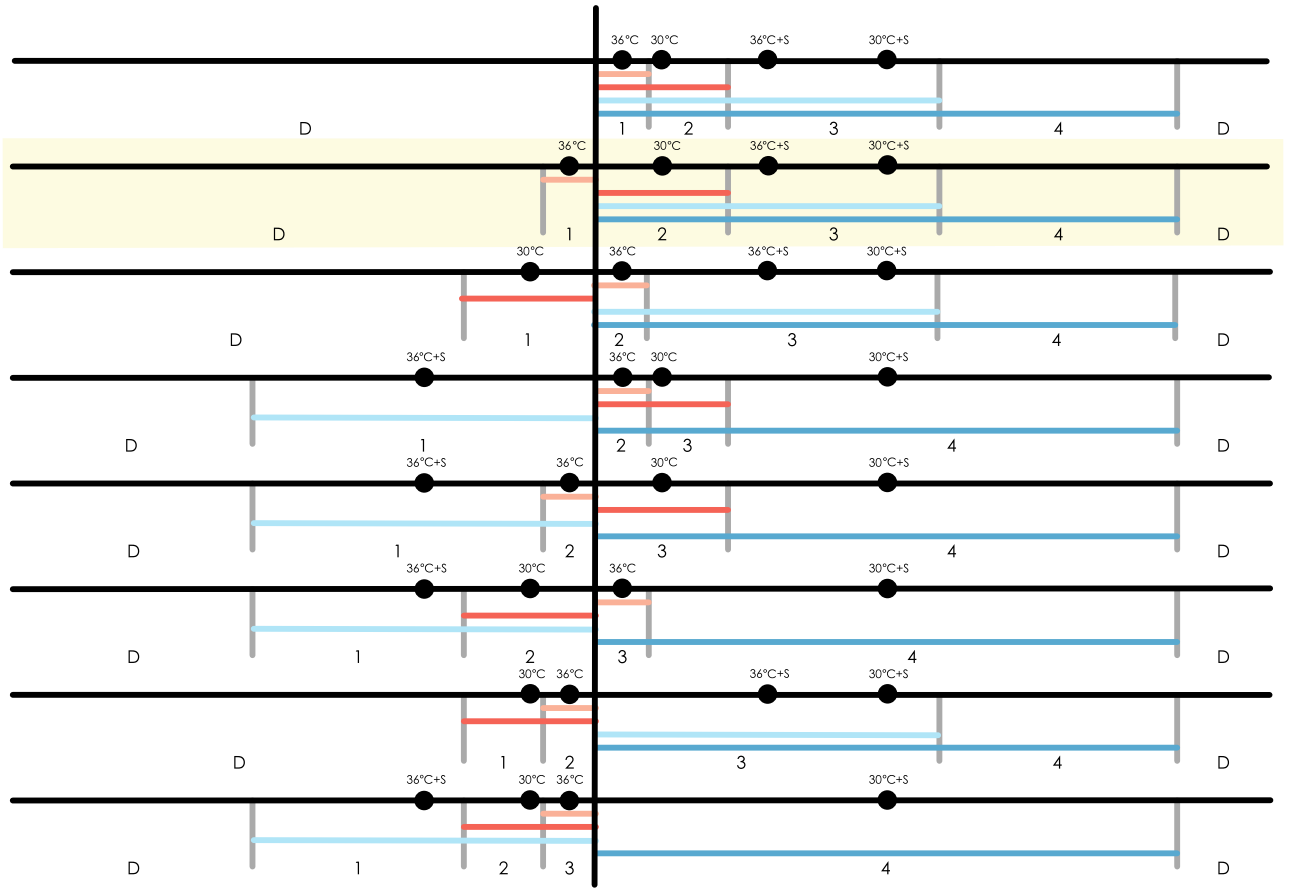


**Figure 5.** **All possible realizations of the FGM in a one-dimensional phenotype space. Horizontal black solid lines represent the phenotype space, whereas the vertical solid black line indicates the position of the current phenotype. For each environment, an interval (representing the one-dimensional version of what is commonly drawn as a circle in the two-dimensional FGM) is drawn as a colored line that spreads from the current phenotype along the phenotype space to twice the distance between the current phenotype and the phenotypic optimum (indicated as indexed black dot) for that environment. This interval represents the area in which mutations have to fall according to a one-dimensional FGM to decrease the distance to the optimum and hence to be beneficial. All eight combinatory possibilities to realize this model are shown, with the second one (highlighted in yellow) representing the best fit that is elaborated in Figure 4. Every realization contains five categories of mutations (D, 1–4) that are characterized by the overlap of colored intervals.**

under the assumption that the DFE follows a shifted gamma distribution. We further observe high costs of adaptation. In particular, mutations that were found to be beneficial in 30°C + S (represented by dark blue background in the histogram in Fig. 3A) are very likely to be deleterious in the low-salinity environments (as indicated by dark blue bars in Fig. 3B,C).

We were interested in the question of whether the observed costs of adaptation are corresponding with the predictions of an FGM that is extended to more than one environment. Roughly, this idea has been sketched in Figure 7 (but see also Fig. 4) of Martin and Lenormand (2006b), if different phenotypic optima characterizing the fitness peaks for different environments are drawn in a phenotype space according to the FGM, subsets of the phenotype space arise in which mutations are deleterious in one but beneficial in the other environment. Hence, as soon as two environments have differently located optima, costs of adaptation are predicted. Moreover, this is necessarily true for every choice of two environments that represent different distances between the current phenotype and the optimum (e.g., standard environment vs adaptive challenge). Here, we do not fit explicit distributions to the DFEs for individual environments. Instead, we use a simplified FGM that reduces the information for each mutant to the sign of its selection coefficient—which indicates its rough location in phenotype space as compared with the current phenotype and the optimum. By comparing this location between environments we can test whether there is a configuration of the FGM (i.e., an arrangement of the current phenotype and the four different optima) that is in accordance with our observed costs of adaptation (which is determined by the sign effect of a mutation in all four environments). To determine the effective number of dimensions of the phenotype space, we use the results of Martin and Lenormand (2006a). Our data for the standard environment yielded

$n_e = 1.08$, which is in concordance with previously published genome-wide values for S. cerevisiae (Martin and Lenormand 2006a). In addition, we estimated the distances to the optimum under the assumption that the DFE (neglecting the deleterious mode with $s <= -0.5$) follows a shifted gamma distribution as suggested by Martin and Lenormand (2006b) (further detailed in Materials and Methods). Mutations were categorized according to the sign of their selection coefficient in each of the four environments, resulting in 16 possible categories of mutations—however, any possible geometric arrangement according to a one-dimensional FGM as defined for our purpose contains only five categories of mutations, which are determined by the ranking of the distances to the optimum (which we fixed according to the estimated distances) and the arrangement of the optima in phenotype space (cf. Fig. 4). This resulted in eight possible models that are consistent with the FGM (cf. Fig. 5). A particular FGM arrangement harbors a chosen mutation if it includes the mutation's category. Despite the restriction on the dimensionality (i.e., on the number of mutational categories allowed), our best fit pursuant to our simplified version of the FGM (graphically represented in Fig. 4) harbors 95.8% of all mutations (99.5% if the sign of mutations that were previously categorized as wt-like are neglected). In addition, we compared the eight models that are compatible with an arrangement according to our definition of the FGM (cf. Fig. 5) with fits to all 4368 possible subsets containing 5 out of 16 mutational categories (i.e., all alternative models with the same complexity, but not compatible with an FGM-like geometrical arrangement). We find that our best fit ranks second among all models, where the overall best model harbors 97.4% of all observed mutations. Furthermore, all eight models that are in concordance with the FGM are within the best 5% of all models, harboring between 79.9% and 95.8% of mutations.

## Conclusions

Many of the greatest accomplishments of the genomic era come from the empirical evaluation of the fundamental theoretical models of evolution proposed nearly a century ago by the founders of the field—Fisher, Haldane, and Wright (for an excellent overview of the early field, see Crow 1987). It is in this vein that we have evaluated FGM. We have experimentally observed many of Fisher's expectations regarding adaptive step sizes as they relate to a population's distance from the optimum state.

Our observations suggest a number of noteworthy implications. First, we observe a striking number of beneficial mutations in a small region of an essential protein. This demonstrates that genomic regions under high constraint harbor hitherto unrecognized potential for adaptation upon environmental change. Interpreting these identified beneficial mutations in light of the known biology of Hsp90, suggests that biochemical context well predicts adaptive response, implying an important role of regulators in dictating adaptive potential. Although this region of Hsp90 is strongly conserved in eukaryotes (Hietpas et al. 2011), some of the salt beneficial mutations that we observed experimentally (e.g., S586T and N588H) are also found in nature. Second, the simple framework of the FGM is sufficient to explain important aspects of our data. In particular, the observed costs of adaptation and the number of shared beneficial mutations between the two high-salinity environments are remarkably consistent with a one-dimensional FGM. And while it is far from conclusive, the repeated observation that beneficial mutations in one environment tend to be mildly to strongly deleterious in all other environments, ought to serve as a note of caution against recent arguments (Hermisson and Pennings 2005; Karasov et al. 2010; Hernandez et al. 2011) for the pervasive role of standing variation in adaptation. Third, we observe that the potential for adaptation is reduced in the combined high temperature and salinity as compared with the high-salinity environment. Combined with the experimental observation that this joint environment also results in the greatest reduction in growth rate, this result is shown to be consistent with the expectation of the FGM. Further, this observation echoes the notion of Haldane (1957), who suggested the difficulty inherent in simultaneous selection for multiple traits.

### ACKNOWLEDGMENTS

This work was supported in part by grants from the National Institutes of Health (R01-GM083038) and the American Cancer Society (RSG-08-17301-GMC) to DNAB, and by grants from the Swiss National Science Foundation and a European Research Council (ERC) Starting Grant to JDJ. We would like to thank vital-IT and the Swiss Institute of Bioinformatics (SIB) for computational resources. The authors declare no conflict of interest.

### LITERATURE CITED

Andolfatto, P. 2007. Hitchhiking effects of recurrent beneficial amino acid substitutions in the *Drosophila melanogaster* genome. Genome Res. 17:1755–1762.

Berry, D. B., and A. P. Gasch. 2008. Stress-activated genomic expression changes serve a preparative role for impending stress in yeast. Mol. Biol. Cell 19:4580–4587.

Borkovich, K. A., F. W. Farrelly, D. B. Finkelstein, J. Taulien, and S. Lindquist. 1989. hsp82 is an essential protein that is required in higher concentrations for growth of cells at higher temperatures. Mol. Cell. Biol. 9:3919–3930.

Boyko, A. R., S. H. Williamson, A. R. Indap, J. D. Degenhardt, R. D. Hernandez, K. E. Lohmueller, M. D. Adams, S. Schmidt, J. J. Sninsky, S. R. Sunyaev, et al. 2008. Assessing the evolutionary impact of amino acid mutations in the human genome. PLoS Genet. 4:e1000083.

Causton, H. C., B. Ren, S. S. Koh, C. T. Harbison, E. Kanin, E. G. Jennings, T. I. Lee, H. L. True, E. S. Lander, and R. A. Young. 2001. Remodeling of yeast genome expression in response to environmental changes. Mol. Biol. Cell 12:323–337.

Crow, J. F. 1987. Anecdotal, historical and critical commentaries on genetics twenty-five years ago in genetics: motoo kimura and molecular evolution. Genetics 116:183–184.

Dhar, R., R. Sagesser, C. Weikert, J. Yuan, and A. Wagner. 2011. Adaptation of *Saccharomyces cerevisiae* to saline stress through laboratory evolution. J. Evol. Biol. 24:1135–1153.

Ewing, B., and P. Green. 1998. Base-calling of automated sequencer traces using phred. II. Error probabilities. Genome Res. 8:186–194.

Ewing, B., L. Hillier, M. C. Wendl, and P. Green. 1998. Base-calling of automated sequencer traces using phred. I. Accuracy assessment. Genome Res. 8:175–185.

Eyre-Walker, A., and P. D. Keightley. 2007. The distribution of fitness effects of new mutations. Nat. Rev. Genet. 8:610–618.

Eyre-Walker, A., M. Woolfit, and T. Phelps. 2006. The distribution of fitness effects of new deleterious amino acid mutations in humans. Genetics 173:891–900.

Fisher, R. 1930. The genetical theory of natural selection. Oxford Univ. Press, Oxford, U.K.

Gasch, A. P., P. T. Spellman, C. M. Kao, O. Carmel-Harel, M. B. Eisen, G. Storz, D. Botstein, and P. O. Brown. 2000. Genomic expression programs in the response of yeast cells to environmental changes. Mol. Biol. Cell 11:4241–4257.

Gietz, R. D., and R. H. Schiestl. 2007. Large-scale high-efficiency yeast transformation using the LiAc/SS carrier DNA/PEG method. Nat. Protoc. 2:38–41.

Gietz, R. D., R. H. Schiestl, A. R. Willems, and R. A. Woods. 1995. Studies on the transformation of intact yeast cells by the LiAc/SS-DNA/PEG procedure. Yeast 11:355–360.

Gresham, D., M. M. Desai, C. M. Tucker, H. T. Jenq, D. A. Pai, A. Ward, C. G. DeSevo, D. Botstein, and M. J. Dunham. 2008. The repertoire and dynamics of evolutionary adaptations to controlled nutrient-limited environments in yeast. PLoS Genet. 4:e1000303.

Haldane, J. B. S. 1957. The cost of natural selection. J. Genet. 55:511–524.

Harris, S. F., A. K. Shiau, and D. A. Agard. 2004. The crystal structure of the carboxy-terminal dimerization domain of htpG, the *Escherichia coli* Hsp90, reveals a potential substrate binding site. Structure 12:1087–1097.

Hawle, P., D. Horst, J. P. Bebelman, X. X. Yang, M. Siderius, and S. M. van der Vies. 2007. Cdc37p is required for stress-induced high-osmolarity glycerol and protein kinase C mitogen-activated protein kinase pathway functionality by interaction with Hog1p and Slt2p (Mpk1p). Eukaryot. Cell 6:521–532.

Hermisson, J., and P. S. Pennings. 2005. Soft sweeps: molecular population genetics of adaptation from standing genetic variation. Genetics 169:2335–2352.

Hernandez, R. D., J. L. Kelley, E. Elyashiv, S. C. Melton, A. Auton, G. McVean, G. Sella, and M. Przeworski. 2011. Classic selective sweeps were rare in recent human evolution. Science 331:920–924.

Hietpas, R., B. Roscoe, L. Jiang, and D. N. Bolon. 2012. Fitness analyses of all possible point mutations for regions of genes in yeast. Nat. Protoc. 7:1382–1396.

Hietpas, R. T., J. D. Jensen, and D. N. Bolon. 2011. Experimental illumination of a fitness landscape. Proc. Natl. Acad. Sci. USA 108:7896–7901.

Hohmann, S. 2002. Osmotic stress signaling and osmoadaptation in yeasts. Microbiol. Mol. Biol. Rev. 66:300–372.

Jensen, J. D., K. R. Thornton, and P. Andolfatto. 2008. An approximate Bayesian estimator suggests strong, recurrent selective sweeps in *Drosophila*. PLoS Genet. 4:e1000198.

Karasov, T., P. W. Messer, and D. A. Petrov. 2010. Evidence that adaptation in *Drosophila* is not limited by mutation at single sites. PLoS Genet. 6:e1000924.

Kassen, R., and T. Bataillon. 2006. Distribution of fitness effects among beneficial mutations before selection in experimental populations of bacteria. Nat. Genet. 38:484–488.

Keightley, P. D., and A. Eyre-Walker. 2007. Joint inference of the distribution of fitness effects of deleterious mutations and population demography based on nucleotide polymorphism frequencies. Genetics 177:2251–2261.

Lalic, J., J. M. Cuevas, and S. F. Elena. 2011. Effect of host species on the distribution of mutational fitness effects for an RNA virus. PLoS Genet. 7:e1002378.

Li, H., and W. Stephan. 2006. Inferring the demographic history and rate of adaptive substitution in *Drosophila*. PLoS Genet. 2:e166.

MacLean, R. C., and A. Buckling. 2009. The distribution of fitness effects of beneficial mutations in *Pseudomonas aeruginosa*. PLoS Genet. 5:e1000406.

Macpherson, J. M., G. Sella, J. C. Davis, and D. A. Petrov. 2007. Genomewide spatial correspondence between nonsynonymous divergence and neutral polymorphism reveals extensive adaptation in *Drosophila*. Genetics 177:2083–2099.

Macpherson, J. M., J. Gonzalez, D. M. Witten, J. C. Davis, N. A. Rosenberg, A. E. Hirsh, and D. A. Petrov. 2008. Nonadaptive explanations for signatures of partial selective sweeps in *Drosophila*. Mol. Biol. Evol. 25:1025–1042.

Manna, F., R. Gallet, G. Martin, and T. Lenormand. 2012. The high-throughput yeast deletion fitness data and the theories of dominance. J. Evol. Biol. 25:892–903.

Martin, G., and T. Lenormand. 2006a. A general multivariate extension of Fisher's geometrical model and the distribution of mutation fitness effects across species. Evolution 60:893–907.

Martin, G., and T. Lenormand. 2006b. The fitness effect of mutations across environments: a survey in light of fitness landscape models. Evolution 60:2413–2427.

Martin, G., S. F. Elena, and T. Lenormand. 2007. Distributions of epistasis in microbes fit predictions from a fitness landscape model. Nat. Genet. 39:555–560.

Martin, G., and T. Lenormand. 2006. A general multivariate extension of Fisher's geometrical model and the distribution of mutation fitness effects across species. Evolution 60:893–907.

McKenzie, S. L., S. Henikoff, and M. Meselson. 1975. Localization of RNA from heat-induced polysomes at puff sites in *Drosophila melanogaster*. Proc. Natl. Acad. Sci. USA 72:1117–1121.

Muller, H. J. 1950. Evidence of the precision of genetic adaptation. Harvey Lect. Ser. 43:165–229.

Ohta, T. 1971. Evolutionary rate of cistrons and DNA divergence. J. Mol. Evol. 1:150–157.

Orr, H. 1998. The population genetics of adaptation: the distribution of factors fixed during adaptive evolution. Evolution 52:935–949.

———. 2003. A minimum on the mean number of steps taken in adaptive walks. J. Theor. Biol. 220:241–247.

Schenk, M. F., I. G. Szendro, J. Krug, and J. A. de Visser. 2012. Quantifying the adaptive potential of an antibiotic resistance enzyme. PLoS Genet. 8:e1002783.

Timofeeff-Ressovsky, N. W. 1940. Mutations and geographical variation. Clarendon Press, Oxford, U.K.

Trindade, S., A. Sousa, and I. Gordo. 2012. Antibiotic resistance and stress in the light of Fisher's model. Evolution 66:3815–3824.

Vale, P. F., M. Choisy, R. Froissart, R. Sanjuan, and S. Gandon. 2012. The distribution of mutational fitness effects of phage phiX174 on different hosts. Evolution 66:3495–3507.

Whitesell, L., and S. L. Lindquist. 2005. HSP90 and the chaperoning of cancer. Nat. Rev. Cancer 5:761–772.

Whitesell, L., E. G. Mimnaugh, B. De Costa, C. E. Myers, and L. M. Neckers. 1994. Inhibition of heat shock protein HSP90-pp60v-src heteroprotein complex formation by benzoquinone ansamycins: essential role for stress proteins in oncogenic transformation. Proc. Natl. Acad. Sci. USA 91:8324–8328.

Yang, X. X., K. C. Maurer, M. Molanus, W. H. Mager, M. Siderius, and S. M. van der Vies. 2006. The molecular chaperone Hsp90 is required for high osmotic stress response in *Saccharomyces cerevisiae*. FEMS Yeast Res. 6:195–204.

Yang, X. X., P. Hawle, J. P. Bebelman, A. Meenhuis, M. Siderius, and S. M. van der Vies. 2007. Cdc37p is involved in osmoadaptation and controls high osmolarity-induced cross-talk via the MAP kinase Kss1p. FEMS Yeast Res. 7:796–807.

Zou, J., Y. Guo, T. Guettouche, D. F. Smith, and R. Voellmy. 1998. Repression of heat shock transcription factor HSF1 activation by HSP90 (HSP90 complex) that forms a stress-sensitive complex with HSF1. Cell 94:471–480.

Associate Editor: A. De Visser

## *Supporting Information*

Additional Supporting Information may be found in the online version of this article at the publisher's website:

**Figure S1.** Growth of wild-type Hsp90 in the four investigated environmental conditions.

**Figure S2.** Fitness effects of synonymous substitutions for the ten amino acid substitutions with the greatest benefit in elevated salinity.

**Figure S3.** Correlation between biological replicates at elevated salinity (30°C + S).

**Figure S4.** Schematic of qPCR based analyses of selection coefficients.

**Figure S5.** Fitness measurements made by binary competition correlate with EMPIRIC results.

**Data S1.** Observed selection coefficients.